Heronamides A–C, new polyketide macrolactams from an Australian marine-derived *Streptomyces* sp. A biosynthetic case for synchronized tandem electrocyclization†

Ritesh Raju, Andrew M. Piggott, Melissa M. Conte and Robert J. Capon*

Received 16th June 2010, Accepted 22nd July 2010
DOI: 10.1039/c0ob00267d

A *Streptomyces* sp. isolated from a shallow water sediment sample collected off Heron Island, Australia, afforded three new polyketide macrolactams, heronamides A–C (**1–3**). Structures were assigned to the heronamides on the basis of detailed spectroscopic analysis, chemical derivatization and biosynthetic considerations. A plausible biosynthetic pathway is proposed in which key carbocyclic ring transformations proceed *via* an unprecedented synchronized tandem electrocyclization. This biosynthesis provides a framework for the assignment of complete relative configurations across all heronamides, and inspires an attractive biomimetic strategy for future total syntheses. Heronamide C elicits a dramatic and reversible non-cytotoxic effect on mammalian cell morphology.

Introduction

Marine-derived actinomycetes are an excellent source of natural products with diverse and unusual carbon skeletons and chemical functionality. Such metabolites provide insights into the broader biosynthetic landscape, revealing new structure classes and biosynthetic pathways, inspiring innovative biomimetic approaches to total synthesis, and displaying valuable biological properties that hold out the prospect of new research probes, medical therapeutics and agrochemicals. Recent examples of novel marine-derived actinomyces metabolites reported from our laboratory include the diketopiperazine naseseazines from a Fijian *Streptomyces* sp.,[1] that highlight biomimetic options for diketopiperazine dimerization, and the macrolide polyketide nocardiopsins from an Australian *Nocardiopsis* sp.,[2] the first members of the rapamycin-like class of FKBP-12 binding polyketide natural products to be described in over a decade. In a continuation of our studies, we now report a series of polyketide macrolactams, heronamides A–C (**1–3**), produced by a *Streptomyces* sp. (CMB-M0406) isolated from shallow-water sediment (−1 m) collected off Heron Island, Australia. In addition to describing the isolation, characterization and structure elucidation of the heronamides as new examples of a rare class of polyketide 20-membered macrolactams featuring unprecedented carbon/heteroatom skeletons, we propose a novel biosynthetic relationship employing a synchronous tandem electrocyclization, supportive of stereochemical assignments and suggestive of a novel biomimetic synthetic strategy.

Institute for Molecular Bioscience, The University of Queensland, St. Lucia, Queensland, Australia, 4072. E-mail: r.capon@uq.edu.au; Fax: +617 3346 2090; Tel: +617 3346 2979

† Electronic supplementary information (ESI) available: Tabulated NMR data and ^{1}H spectra for all compounds. See DOI: 10.1039/c0ob00267d

Results and Discussion

Chemical analysis of saline and non-saline liquid fermentations (100 mL) of a *Streptomyces* sp. (CMB-M0406) isolated from shallow-water sediment collected off Heron Island, Australia, revealed media-selective biosynthesis of unusual nitrogenous polyenes (Fig. 1, m/z (M+Na)$^+$ 488 (**1**), 472 (**2**) and 472 (**3**)). The polyenes detected in these fermentations were isolated and identified by fractionation of a larger-scale saline liquid fermentation

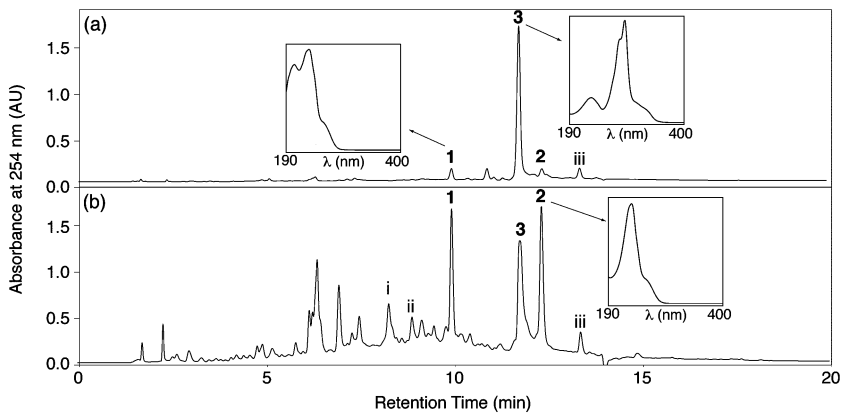

Fig. 1 C_8 HPLC traces of (a) non-saline and (b) saline liquid fermentations of a *Streptomyces* sp. (CMB-M0406), with UV-vis inserts of heronamides A–C (**1–3**) extracted from diode array detector. Putative heronamide analogs i (MW 499), ii (MW 481) and iii (MW 433) are also indicated.

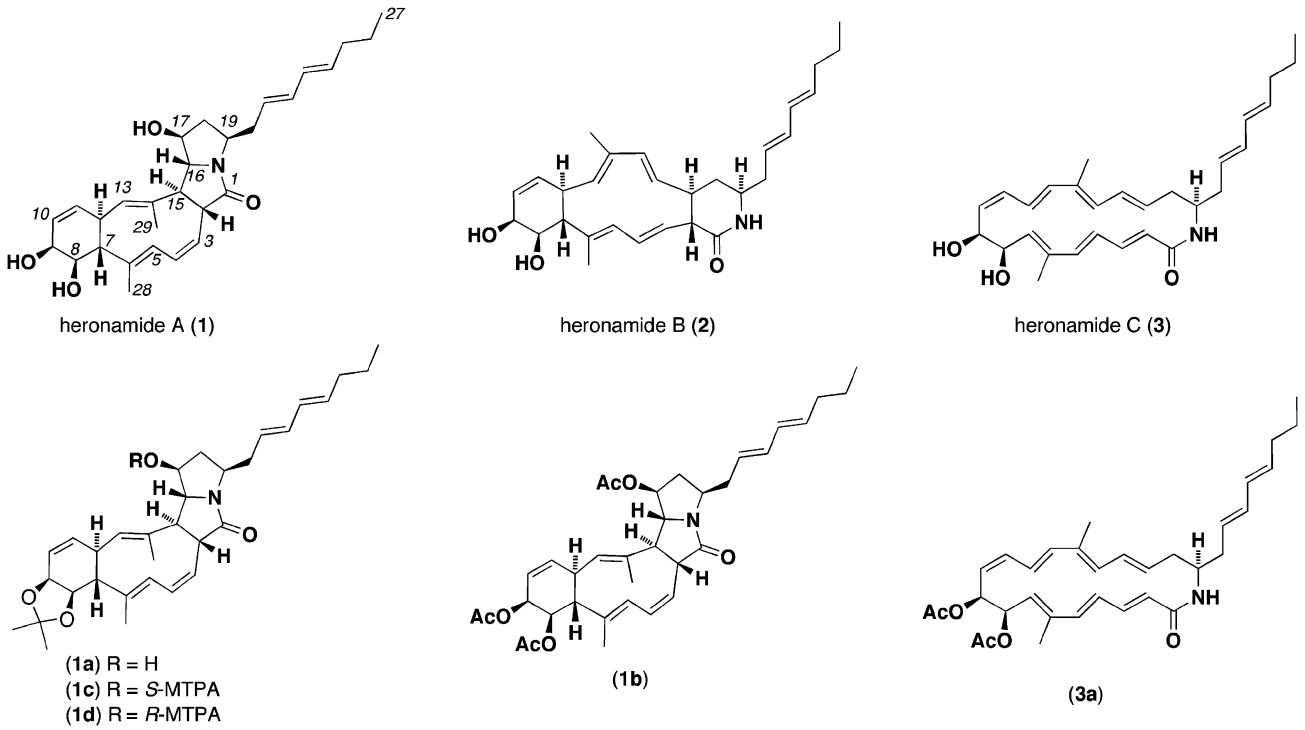

Fig. 2 Heronamides A–C (**1–3**) and synthetic derivatives.

(3 L), employing sequential solvent partitioning and trituration, followed by reversed phase HPLC. This process yielded three new polyketide macrolactams, identified as heronamides A–C (**1–3**) (Fig. 2).

The HRESI(+)MS data for heronamide A (**1**) returned a pseudomolecular ion $(M+Na)^+$ consistent with a molecular formula ($C_{29}H_{39}NO_4$, Δmmu −0.6) requiring eleven double bond equivalents (DBE). The ^{13}C NMR (methanol-d_4) data for **1** (Table 1 and ESI Table S1†) displayed resonances for a single ester/amide carbonyl (δ_C 177.3) and twelve sp^2 olefinic carbons (δ_C 125.4 to 137.8), accounting for seven DBE and requiring that **1** be tetracyclic. The 1D NMR data also indicated one primary methyl (δ_H 0.92, t, J 7.4 Hz; δ_C 13.9) and two olefinic methyls (δ_H 1.75, s and 1.41, s; δ_C 12.6 and 16.8), which served as useful points of reference for interpretation of the 2D NMR data (Fig. 3). For example, a correlation sequence extended from the primary methyl (C-27) through two methylenes, a conjugated disubstituted diene (E $\Delta^{21,22}$ $J_{21,22}$ 14.8 Hz; E $\Delta^{23,24}$ $J_{23,24}$ 14.5 Hz), to a diastereotopic methylene – consistent with subunit A (C-20 to C-27, Fig. 3).

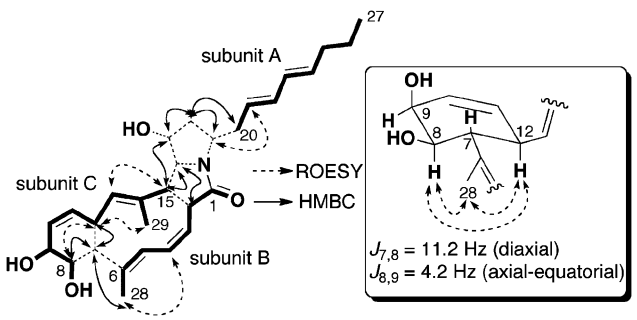

Fig. 3 Key NMR (methanol-d_4) correlations for **1**.

A second correlation sequence positioned an olefinic methyl (C-28) on a conjugated diene (Z $\Delta^{3,4}$, $J_{3,4}$ 10.8 Hz; E $\Delta^{5,6}$, H_3-28 to H-4 ROESY correlation and C-28, δ_C 12.6), attached through a deshielded methine to the ester/amide carbonyl (C-1) – consistent with subunit B (C-1 to C-6, Fig. 3). A third correlation sequence positioned an olefinic methyl (C-29) on an trisubstituted double bond (E $\Delta^{13,14}$, H_3-29 to H-12 ROESY correlation and C-29, δ_C 16.8), with further connections through a deshielded bisallylic methine to a disubstituted double bond (Z $\Delta^{10,11}$, H-8 to H-12 ROESY correlation), extending through a deshielded oxymethine to a second oxymethine – consistent with subunit C (C-8 to C-15, Fig. 3).

Although the ^1H NMR resonances for H-7 and H_2-25 were overlapping, HMBC correlations from H_3-28, H-8 and H-12 to C-7 unambiguously connected subunits B and C, and established the C-7 to C-12 cyclohexenyl moiety. Relative configurations about the cyclohexenyl moiety were evident from ROESY correlations, together with $J_{8,9}$ (4.2 Hz), as indicated in Fig. 3. Further COSY correlations between H-2 and H-15, supported by HMBC correlations linking H-2 to C-15, and H-15 to C-2, C-3 and C-4, established the macrocycle as indicated. In summary, subunits A–C account for all but C_4H_6ON and 2 DBE, suggesting that the remaining structural feature be a bicyclic heterocycle. Further analysis of the NMR data identified several components of this subunit as a methylene (C-18), three heteroatom deshielded methines (C-16, C-17 and C-19), and by inference an exchangeable proton (either an O*H* or N*H*). Although the ^1H NMR resonances for the three methines H-16, H-17 and H-19 were overlapping, the corresponding ^{13}C NMR resonances were resolved and provided valuable structural information. For example, HMBC correlations from H_2-18 to C-17 and C-19, and from H-15 to C-16 and C-17, established the sequence C-15 to C-19, while correlations from

Table 1 NMR data for heronamides A–C (**1–3**)

	heronamide A (**1**) in methanol-d_4		heronamide B (**2**) in methanol-d_4		heronamide C (**3**) in pyridine-d_5	
pos	δ_H, mult (*J* in Hz)	δ_C	δ_H, mult (*J* in Hz)	δ_C	δ_H, mult (*J* in Hz)	δ_C
1		177.3		175.5		168.3
2	3.64, ddd (9.2, 7.2, 2.4)	55.6	2.68, dd (10.5, 10.1)	56.0	6.34, m[a]	129.9
3	5.45, dd (10.8, 7.2)	125.4	5.05, dd (15.1, 10.1)	130.8	7.38, dd (14.9, 11.0)	141.5
4	6.68, ddd (10.8, 9.8, 2.4)	133.4	5.92, dd (15.1, 11.0)	135.4	6.22, m[a]	125.5
5	5.51, d (9.8)	130.7	5.63, m[a]	134.2	6.36, m[a]	143.9
6		132.9		135.5		132.5
7	2.07, m[a]	53.6	2.33, m[a]	55.7	5.84, br d (8.2)	140.0
8	3.84, dd (11.4, 4.2)	70.8	3.81, dd (11.6, 4.2)	71.4	5.33, dd (8.2, 3.0)	73.4
9	4.12, dd (4.8, 4.2)	67.7	4.13, m	67.9	5.01, dd, (8.9, 3.0)	71.5
10	5.87, m[a]	128.1	5.81, m[a]	128.3	6.18, m[a]	132.6
11	5.88, m[a]	133.6	5.81, m[a]	134.4	6.33, m[a]	124.4
12	2.82, m	43.7	3.18, dd (10.5, 9.7)	43.6	6.24, m[a]	124.7
13	5.05, d (10.8)	133.1	4.86[b]	133.8	6.21, m[a]	137.4
14		137.8		137.8		133.7
15	3.22, dd (9.2, 8.6)	59.0	5.73, d (16.0)	142.1	6.11, d (11.4)	131.3
16	3.90, m[a]	68.5	4.96, dd (16.0, 9.7)	127.3	6.51, dd (14.9, 11.4)	131.3
17	3.89, m[a]	76.0	2.42, m	47.4	5.88, ddd (14.9, 10.5, 5.4)	131.2
18α	2.50, m[a]	42.3	2.15, ddd (13.3, 4.8, 2.6)	34.8	2.53, m	34.8
18β	1.81, ddd (13.1, 7.8, 7.8)		1.60, m		2.07, dd (23.1, 10.5)	
19	3.91, m[a]	53.3	3.56, m	53.7	4.56, m	50.4
20a	2.46, m[a]	37.9	2.31, m[a]	40.7	2.45, ddd (14.3, 7.3, 7.1)	39.0
20b	2.43, m[a]				2.39, ddd (14.3, 7.1, 6.7)	
21	5.57, dt (14.8, 7.5)	126.7	5.54, dt (15.0, 7.4)	126.6	5.77, dt (15.1, 7.1)	128.9
22	6.12, dd (14.8, 10.4)	135.2	6.14, dd (15.0, 10.4)	135.5	6.19, m[a]	133.2
23	6.05, dd (14.5, 10.4)	131.4	6.05, dd (15.0, 10.4)	131.3	6.02, dd (14.8, 10.3)	131.1
24	5.64, dt (14.5, 7.2)	134.1	5.65, m[a]	134.5	5.58, dt, (14.8, 6.9)	133.1
25	2.06, m[a]	35.6	2.06, m	35.6	1.96, td (7.5, 6.9)	34.8
26	1.42, sxt (7.4)	23.5	1.41, m	23.5	1.30, sxt, (7.5)	22.7
27	0.92, t (7.4)	13.9	0.92, t (7.4)	13.9	0.81, t (7.5)	13.8
28	1.75, s	12.6	1.69, s	13.1	1.77, s	12.7
29	1.41, s	16.8	1.64, s	14.1	1.72, s	12.5
NH					7.98, d (10.3)	

[a] Overlapping signals. [b] Obscured by H_2O signal. Assignments supported by 2D NMR analyses (HSQC, HMBC, COSY, ROESY).

H_2-20 to C-19 and C-18 positioned subunit A as a substituent to C-19 (Fig. 3). Nevertheless, the NMR data for **1** did not allow the unambiguous identification of the heterocyclic subunit.

To achieve better dispersion of NMR signals, and hopefully unambiguously identify the heterocyclic core, we prepared two derivatives, heronamide A acetonide (**1a**) and heronamide A triacetate (**1b**). Formation of the acetonide **1a** (ESI Table S4†, δ_H 1.40, s, H_3-30; 1.38, s, H_3-31; $J_{7,8}$ 11.1 Hz and $J_{8,9}$ 6.0 Hz) confirmed the presence of a *cis*-8,9-diol functionality, consolidating structure elucidation of the cyclohexenyl moiety as presented above. Formation of the tri-*O*-acetate **1b** (ESI Table S5a†, δ_H 1.98, s, 9-OAc; 2.03, s, 17-OAc; 2.07, s, 8-OAc) further reinforced structure assignment of the cyclohexenyl moiety, while also being supportive of a C-17 secondary hydroxyl. The NMR data for the heterocyclic subunit in the triacetate **1b** was better resolved than that of **1**, and permitted ready assignment of the planar structure and relative configuration. For example, 2D COSY NMR (methanol-d_4) correlations (ESI Table S5a, Fig. 4†) established a connectivity sequence from H-15, through H-16, H-17, H_2-18 and H-19, to H_2-20, while ROESY correlations position H-17, H-18α and H-19 on one face, and H_3-29, H-16 and H-18β on the other face of the heterocyclic system. Analysis of the ^{1}H NMR ($CDCl_3$) data (ESI Table S5b†) revealed H-17 (previously obscured by residual MeOH in methanol-d_4), allowing unambiguous measurement of $J_{2,15}$ (8.9 Hz), which was suggestive

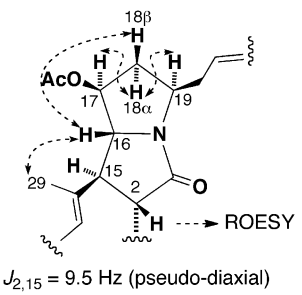

Fig. 4 Key NMR (methanol-d_4) correlations for heterocyclic subunit in **1b**.

of a pseudo-diaxial relationship. Collectively, these analyses of the derivatives **1a** and **1b** permitted assignment of the complete relative configuration about the heterocyclic subunit. Based on the arguments presented above, the structure for heronamide A (**1**) (and the derivatives **1a** and **1b**) was proposed as shown (less absolute stereochemistry). The relative configuration between the cyclohexenyl and heterocyclic subunits was tentatively assigned on consideration of a likely biosynthetic relationship to heronamide C (**3**), involving a synchronous 4π+6π tandem electrocyclization (discussed later).

In our hands, heronamide B (**2**) co-eluted under several HPLC conditions with a saturated *iso*-fatty acid co-metabolite that

was identified by spectroscopic analysis and comparison with authentic standards as isomyristic acid ($C_{14}H_{28}O_2$). The co-elution of isomyristic acid notwithstanding, the HRESI(+)MS data for **2** returned a pseudomolecular ion $(M+Na)^+$ consistent with a molecular formula ($C_{29}H_{39}NO_3$, Δmmu –0.6) requiring eleven DBE. The ^{13}C NMR (methanol-d_4) data (Table 1 and ESI Table S2†) displayed resonances for a single ester/amide carbonyl (δ_C 175.5) and fourteen sp^2 olefinic carbons (δ_C 126.6 to 142.1), accounting for eight DBE and requiring that **2** be tricyclic. The 1D and 2D NMR resonances and correlations defined the complete carbon skeleton (Fig. 5) and established relative configurations about the double bonds; *E* $\Delta^{3,4}$ ($J_{3,4}$ 15.1 Hz), *E* $\Delta^{5,6}$ (C-28, δ_C 13.1), *Z* $\Delta^{10,11}$ (H-8 to H-12 ROESY correlation), *E* $\Delta^{13,14}$ (C-29, δ_C 14.1), *E* $\Delta^{15,16}$ ($J_{15,16}$ 16.0 Hz), *E* $\Delta^{21,22}$ ($J_{21,22}$ 15.0 Hz) and *E* $\Delta^{23,24}$ ($J_{23,24}$ 15.0 Hz). Relative configurations about the cyclohexenyl subunit were determined to be the same as for heronamide A (**1**) (Fig. 5), with key ^1H–^1H coupling constants and ROESY correlations positioning H-8, H-9, H-12 and H_3-28 on one face, and H-7 and H-13 on the other face of the cyclohexenyl ring. Likewise, the relative configuration about the lactam heterocycle was established by key ^1H–^1H coupling constants and ROESY correlations, which positioned H-3, H-17 and H-19 on one face, and H-2 and H-16 on the other face of the ring system (Fig. 5). Based on the arguments presented above, the structure for heronamide B (**2**) was assigned as shown (less absolute stereochemistry). As with **1**, the relative configuration between the cyclohexenyl and heterocyclic subunits in **2** was tentatively assigned on consideration of a likely biosynthetic relationship to heronamide C (**3**), involving a synchronous 6π+6π tandem electrocyclization (discussed later).

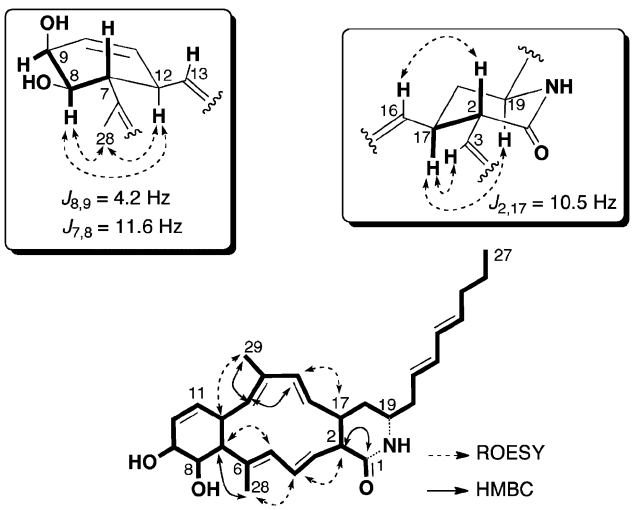

Fig. 5 Key NMR (methanol-d_4) correlations for **2**.

The HRESI(+)MS data for heronamide C (**3**) returned a pseudomolecular ion $(M+Na)^+$ consistent with a molecular formula ($C_{29}H_{39}NO_3$, Δmmu –0.6) isomeric with **2**. Heronamide C (**3**) proved to be difficult to handle and characterize, displaying very poor solubility in a range of common NMR solvents ($CDCl_3$, acetone-d_6, DMSO-d_6 and methanol-d_4). Fortunately, **3** did generate promising 1D and 2D NMR data in pyridine-d_5 (Table 1 and ESI Table S3†), with resonances attributed to a single ester/amide carbonyl (δ_C 168.3) and eighteen sp^2 olefinic carbons (δ_C 124.4 to 143.9) accounting for ten DBE, and requiring that **3** be monocyclic. A more comprehensive analysis of the NMR data revealed resonances and correlations that defined the complete carbon skeleton (Fig. 6) and established relative configurations about several double bonds; *E* $\Delta^{2,3}$ ($J_{2,3}$ 14.9 Hz), *E* $\Delta^{6,7}$ (C-28, δ_C 12.7), *E* $\Delta^{14,15}$ (C-29, δ_C 12.5), *E* $\Delta^{16,17}$ ($J_{16,17}$ 14.9 Hz), *E* $\Delta^{21,22}$ ($J_{21,22}$ 15.1 Hz) and *E* $\Delta^{23,24}$ ($J_{23,24}$ 14.8 Hz).

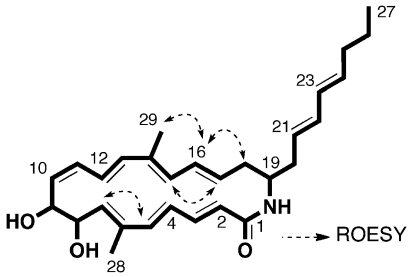

Fig. 6 Key NMR (methanol-d_4) correlations for **3**.

With improved solubility, the NMR (methanol-d_4) data for the diacetate derivative **3a** (ESI Table S6†) displayed improved dispersion that allowed for assignment of *E* $\Delta^{4,5}$ ($J_{4,5}$ 15.1 Hz), *Z* $\Delta^{10,11}$ ($J_{10,11}$ 10.8 Hz) and *E* $\Delta^{12,13}$ ($J_{12,13}$ 15.1 Hz). The complete relative stereochemistry of **3** (inclusive of C-19) was tentatively assigned on consideration of the likely biosynthetic relationship between **3** and the co-metabolites **1** and **2**, as discussed below.

A plausible biosynthetic process linking **1–3** is shown in Fig. 7. In this proposal, **3** is viewed as a pivotal polyene precursor, capable of undergoing either a synchronous 6π+6π tandem electrocyclization to generate **2**, or selective epoxidation and S_N2 mediated macrolactam-pyrrolidine formation, followed by a synchronous 4π+6π tandem electrocyclization, to generate **1**. Significantly, to arrive at the observed *trans*-substitution patterns about the cyclohexenyl (C-7/C-12) and δ-lactam (C-2/C-17) subunits in **2**, we propose that the 6π+6π tandem electrocyclization proceed in a conformational synchronized conrotatory fashion. This requirement effectively links the relative conformations of the cyclohexenyl and δ-lactam subunits, and permits tentative assignment of the complete relative configuration for **2**. By analogy, we propose that the hypothetical macrolactam-pyrrolidine intermediate between **3** and **1** undergoes a comparable conformationally synchronized conrotatory 4π+6π tandem electrocyclization to yield **1**. Again, this requirement provides a conformation bridge across the macrocycle, permitting a tentative assignment of the complete relative configuration for **1**. By corollary, the relative configurations attributed to **2** and **3** about C-8, C-9 and C-19 can be correlated back to the biosynthetic precursor **3**. The biosynthetic analysis described above notwithstanding, we acknowledge that the hypothetical biosynthetic electrocyclizations illustrated in Fig. 7 initially lead to the *Z* conformation about $\Delta^{5,6}$ and $\Delta^{13,14}$. To account for this we suggest that the newly formed contracted ring systems undergo inversion to the more thermodynamically favoured *E* conformation evident in heronamides A (**1**) and B (**2**). Although this biosynthetic proposal remains a hypothesis at this stage, it nevertheless serves as a valuable device to reinforce the biosynthetic merit of the assigned structures, inclusive of stereochemical assignments, while also being suggestive of an attractive biomimetic approach to total synthesis. In summary, using the complementary approaches of spectroscopic analysis, chemical derivatization and biosynthetic

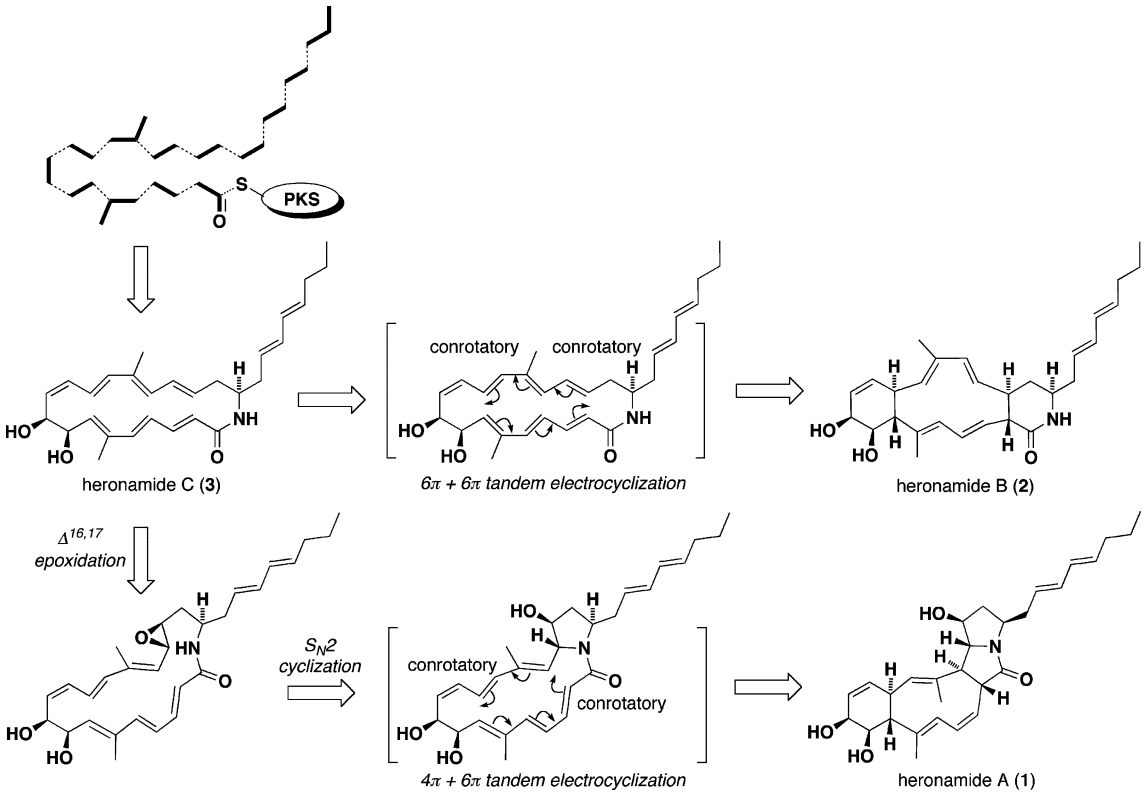

Fig. 7 Plausible biosynthetic relationship between heronamides A–C (**1–3**).

considerations, we propose structures with complete relative configurations for heronamides A–C (**1–3**).

To assign absolute configurations to the heronamides we prepared the *S*-MTPA and *R*-MTPA esters (**1c** and **1d** respectively) of heronamide A acetonide (**1a**), as part of a Mosher analysis.[3] As the available supply of all heronamides and derivatives was limited, the derivatization and subsequent NMR analyses were undertaken *in situ* at an analytical scale (150 μg). The ^{1}H NMR spectra of **1c** and **1d** (ESI Fig. S7a†) revealed a positive $\Delta\delta^{SR}$ for H-16 (+42 Hz) and a negative $\Delta\delta^{SR}$ for H-19 (−30 Hz), confirming a 17*S* configuration for **1a**. By inference, this permitted assignment of absolute configurations to all chiral centres across heronamides A–C and derivatives.

Having successfully identified **1–3**, we returned to the HPLC profiles for the crude saline and non-saline fermentation extracts (Fig. 1) with a view to detecting minor biosynthetically related co-metabolites, possibly supportive of the proposed biosynthesis. This analysis revealed three promising candidates, all of which possessed UV-vis and mass spectral data consistent with heronamide-like polyene macrolactams. More specifically, highlighted peak iii was suggestive of a deoxy analogue of **3**, while ii and i were suggestive of oxy and diol analogues of **1** or **2**.

The heronamides, and their acetonide and acetate derivatives, were evaluated for cytotoxicity and *anti*-proliferative activity against human cancer cell lines (HeLa and MDA-MB-231), as well as growth inhibitory properties against Gram-negative (*Escherichia coli* ATCC 11775) and Gram-positive (*Bacillus subtilis* ATCC 6051; *Staphylococcus aureus* ATCC 25923) bacteria, and a fungus (*Candida albicans*). Although none of the natural products or derivatives displayed anticancer or antibiotic activity, heronamide C (**3**) did elicit an unexpected and dramatic effect on cell morphology (Fig. 8). Human cancer cell lines exposed to **3** (24 h) developed large intracellular structures that dissipated, with no apparent adverse effects, on removal of **3** from the cell media. Given prior interest in polyketide 20-membered macrolactams

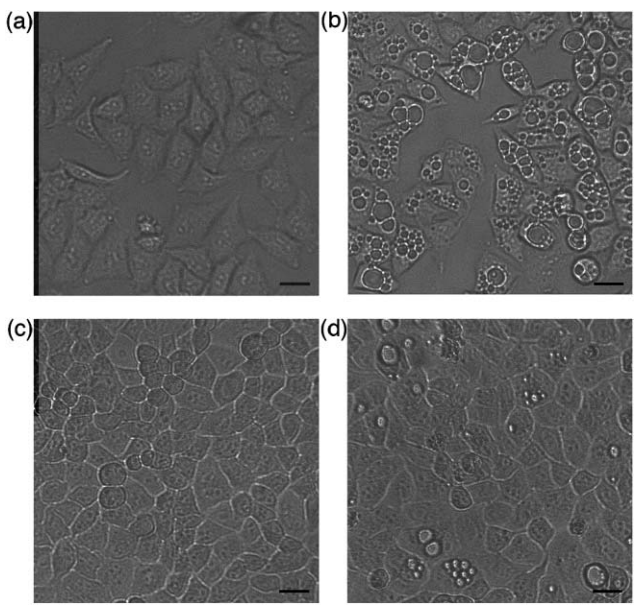

Fig. 8 Light microscope images of HeLa cells after 24 h exposure to (a) 1% DMSO (control) and (b) 50 μM heronamide C (**3**) + 1% DMSO. After being exchanged into fresh media and incubated for 24 h, the (c) control cells and (d) heronamide C-treated cells were reimaged. Black bar = 10 μm.

as antitumor and antibiotic agents, and as treatments of acute and chronic inflammatory disease (see below), the nature and mechanism-of-action behind the effect of **3** on cell morphology is a matter of interest, and is the subject of ongoing investigations.

Polyketide 20-membered macrolactams such as the heronamides are rare and, to the best of our knowledge, published accounts are limited to only seven known examples, all of which are *Streptomyces* metabolites (ESI Fig. S8†). Cyclamenol was patented in 1994 by Bayer, as a leukocyte adhesion inhibitor with application in the treatment of acute and chronic inflammatory diseases.[4] BE-67251 was patented in 2000 as an antitumor agent, by Banyu Pharmaceuticals,[5] and shares a macrolactam-pyrrolidine functionality in common with our hypothetical biosynthetic intermediate linking **3** with **1**. Despite (or possibly because of) commercial value, neither cyclamenol nor BE-67251 is documented in the primary scientific literature, although the total synthesis of an unnatural stereoisomer of cyclamenol has been described.[6,7]

The first polyketide 20-membered macrolactam to appear in the primary scientific literature was BE-14106, reported in 1992 as antitumor antibiotic by researchers from Banyu Pharmaceuticals.[8] BE-14106 was subsequently redescribed in 1997 (as GT32-A) along with the deoxy analogue GT32-B, by researchers from another Japanese company, Kyowa Hakko Kogyo.[9] Both BE-14106 and GT32-B displayed comparable cytotoxic and antibiotic properties, and their structure assignment relied on the spectroscopic analysis of acetate derivatives. The antitumor antibiotic vicenistatin was reported in 1993 by researchers from yet another Japanese company, Kirin Brewery,[10] and its complete absolute stereochemistry was subsequently solved by enantioselective synthesis.[11] The mycarose glycoside analogue, vicenistatin M, was reported in 2001 and provided structure activity relationship information relating to the importance of the aminosugar vicenisamine.[12] Finally, and most recently, ML-449 was reported in 2010 from a marine-derived *Streptomyces* during phylogenetic and evolutionary investigations into the relationship between non-ribosomal peptide synthase (NRPS) and polyketide synthase (PKS) macrolactam gene clusters.[13]

In addition to the 20-membered macrolactams listed above, closely related larger ring macrolactams isolated from marine-derived and marine actinomycetes include the 22-membered aureoverticillactam from *Streptomyces aureoverticillatus*,[14] and the 26-membered salinilactam from *Salinispora tropica*[15] (ESI Fig. S9†). This latter study was particularly noteworthy in that genomic analysis played a significant role in both revealing biosynthetic capability and structure elucidation of the polyketide salinilactam.

Conclusion

The heronamides represent a significant contribution to knowledge of polyketide 20-membered macrolactams, suggestive of a biosynthetic relationship involving an unprecedented synchronous tandem electrocyclization. A characteristic of spectroscopic investigations into *Streptomyces* 20-membered macrolactams has been the complexity of stereochemical analysis, which has typically been restricted to the assignment of double bond configurations. The comprehensive spectroscopic, chemical and biosynthetic investigations described above culminated in the assignment of total absolute stereostructures for all heronamides.

Experimental

General Experimental Details

Chiroptical measurements ($[\alpha]_D$) were obtained on a JASCO P-1010 polarimeter in a 100 × 2 mm cell. UV-visible spectra were obtained on a Cary 50 spectrophotometer in 1 cm quartz cells. IR spectra were obtained on a JASCO FT/IR-460 Plus spectrometer as thin films on CaF_2 plates. NMR spectra were obtained on a Bruker Avance DRX600 spectrometer, in the solvents indicated and referenced to residual ^1H and ^{13}C signals in deuterated solvents. Electrospray ionization mass spectra (ESIMS) were acquired using an Agilent 1100 Series separations module equipped with an Agilent 1100 Series LC/MSD mass detector in both positive and negative ion modes. High-resolution ESIMS measurements were obtained on a Bruker micrOTOF mass spectrometer by direct infusion in MeCN at 3 μL min^{-1} using sodium formate clusters as an internal calibrant. HPLC was performed using an Agilent 1100 Series separations module equipped with Agilent 1100 Series diode array and/or multiple wavelength detectors and Agilent 1100 Series fraction collector, controlled using ChemStation Rev.9.03A and Purify version A.1.2 software.

Isolation and Identification

The bacterium strain CMB-M0406 was cultured from a marine sediment sample collected from a depth of 1 m off Heron Island, Queensland, Australia. Approximately 1 g of the sediment sample was suspended in 4 mL of Ocean Nature seawater (Aquasonic, Australia) and then subjected to heat-shock at 55 °C for 8 min after which 50 μL was transferred on to agar plates (comprising 25 mL of 1% starch, 0.4% yeast extract, 0.2% peptone, 1.8% agar, and 0.0005% rifampicin). A pure culture was obtained for strain CMB-M0406 by repeated, single colony transfer on solid media. Genomic DNA extraction was performed using the DNeasy blood and tissue kit as per the manufacturers protocol. The 16S rRNA genes were amplified from genomic DNA by PCR using primers FC 27 (5′-AGAGTTTGATCCTGGCTCAG-3′) and RC 1492 (5′-TACGGCTACCTTGTTACGACTT-3′). The 50 μL PCR mixture contained 25 to 45 ng of DNA, 250 pmol of each primer, 2.5 U of Taq DNA polymerase and 100 μM deoxynucleoside triphosphate mixture. Amplification products were examined by agarose gel electrophoresis. On the basis of an NCBI BLAST analysis of the 16S rRNA gene sequence of this strain shares more than 99% sequence identity with previously reported *Streptomyces* sp.[13]

Analytical Cultivation and Chemical Profiling

Strain CMB-M0406 was cultivated in two Schott flasks (250 mL) each containing M1 (1% starch, 0.4% yeast extract and 0.2% peptone) with one prepared in distilled water, and the other using Ocean Nature Sea Salt (100 mL). The strains were shaken at 160 rpm for 7 d at 27 °C, extracted with EtOAc (2 × 50 mL per flask), and the organic phases concentrated *in vacuo* to yield crude extracts of 4.6 mg and 3.9 mg respectively. The crude extracts were redissolved in MeOH generating a concentration of 1 mg mL^{-1} and analysed by HPLC-DAD-ESI(±) MS with conditions set a follows (Zorbax C_8 column, 150 × 4.6 mm, 5 μm, 1 mL min^{-1},

gradient from 10–100% MeCN–H_2O (isocratic 0.05% formic acid) over 15 min, with a hold at 100% MeCN for 5 min.

Preparative Cultivation and Chemical Profiling

Six 2 L Erlenmeyer flasks containing M1 broth (500 mL) were inoculated with starter culture (5 mL) of *Streptomyces* sp. (CMB-M0406). The flasks were incubated at 27 °C on a rotary shaker at 190 rpm for 7 d, extracted with EtOAc (2 × 300 mL per flask), and the organic phases concentrated *in vacuo* to yield a combined EtOAc extract (92.3 mg). The EtOAc extract was sequentially triturated with hexane, CH_2Cl_2 and MeOH (25 mL aliquots), which were concentrated *in vacuo*, to yield 22.7 mg, 47.8 mg and 8.7 mg partitions respectively. The CH_2Cl_2 soluble material was further fractionated by HPLC (Zorbax C_8 column, 250 × 9.4 mm, 5 µm, 4 mL min^{-1}, gradient from 10–100% MeOH–H_2O over 40 min) to afford heronamide A (**1**) (t_R = 33.2 min, 2.4 mg, 2.6%), heronamide B (**2**) (t_R = 37.6 min, 1.0 mg, 1.1%) and heronamide C (**3**) (t_R = 34.8 min, 2.0 mg, 2.2%). [Note-% yields are determined on a mass-to-mass basis against the weight of EtOAc crude extract]

Heronamide A (1). Yellow oil; $[\alpha]_D^{20}$ −31 (*c* 0.10 in MeOH); UV (MeOH) λ_{max}/nm (log ε) 227 (4.46); IR (thin film) ν_{max}/cm^{-1} 3348(br), 2926(m), 2360(m), 1670(vs). NMR (600 MHz, methanol-d_4) see Table 1 and ESI Table S1†; HRESI(+)MS *m/z* 488.2771 $(M+Na)^+$ (calcd for $C_{29}H_{39}NO_4Na$, 488.2777).

Heronamide B (2). Yellow oil; contaminated with 30% isomyristic acid, as determined from HRESI(−)MS (*m/z* 227.2017) $(M-H)^-$ calcd for $C_{14}H_{28}O_2$, 227.3630); $[\alpha]_D^{20}$ +31 (*c* 0.10 in MeOH – corrected for 30% achiral i*so*-fatty acid); UV (MeOH) λ_{max}/nm (log ε) 232 (4.50); NMR (600 MHz, methanol-d_4) see Table 1 and ESI Table S2†; HRESI(+)MS *m/z* 472.2822 $(M+Na)^+$ (calcd for $C_{29}H_{39}NO_3Na$, 472.2828).

Heronamide C (3). White powder; $[\alpha]_D^{20}$ +151 (*c* 0.10 in MeOH); UV (MeOH) λ_{max}/nm (log ε) 230 (4.51), 290 (4.47); NMR (600 MHz, pyridine-d_5) see Table 1 and ESI Table S3†; HRESI(+)MS *m/z* 472.2822 $(M+Na)^+$ (calcd for $C_{29}H_{39}NO_3Na$, 472.2828).

Synthesis of Analogs

Heronamide A acetonide (1a). A solution of **1** (2.5 mg, 5.4 µmol), pyridinium-*p*-toluenesulfonate (4 mg, 16 µmol) in 2,2-dimethoxypropane (1 mL) and MeOH (1 mL) was stirred at room temperature for 1 h. The reaction was then quenched with aqueous $NaHCO_3$ (5%; 1 mL), and extracted twice with CH_2Cl_2. The combined organic layer was reduced to dryness *in vacuo* and the residue purified by HPLC (Zorbax C_8 column, 250 × 9.4 mm, 5 µm, 4 mL min^{-1}, gradient from 10–100% MeOH–H_2O over 15 min, with a hold at 100% MeOH for 5 min) to yield the isopropylidene derivative **1a** (t_R = 16.8 min, 0.9 mg, 36%) as a colourless oil (t_R = 16.8 min, $[\alpha]_D^{20}$ −18.9 (*c* 0.09, MeOH); UV (MeOH) λ_{max} (log ε) 228 (4.42); NMR (600 MHz, methanol-d_4) see ESI Table S4†; HRESI(+)MS *m/z* 528.3092 $(M+Na)^+$ (calcd for $C_{32}H_{43}NO_4Na$, 528.3084)

Heronamide A triacetate (1b). A solution of **1** (2.5 mg) in pyridine (300 µL) and acetic anhydride (300 µL) was stirred overnight, after which the reaction was concentrated to dryness, resuspended in MeOH and purified by HPLC (Zorbax C_8 column, 250 × 9.4 mm, 5 µm, 4 mL min^{-1}, gradient from 10–100% MeOH–H_2O over 15 min, with a hold at 100% MeOH for 5 min) to yield the triacetate derivative **1b** (t_R = 17.0 min, 1.1 mg, 44%) as a colourless oil; $[\alpha]_D^{20}$ −9.6 (*c* 0.1, MeOH); UV (MeOH) λ_{max} (log ε) 231 (4.39); NMR (600 MHz, methanol-d_4 and $CDCl_3$) see ESI Tables S5a and S5b†; HRESI(+)MS *m/z* 614.3077 $(M+Na)^+$ (calcd for $C_{35}H_{45}NO_7Na$, 614.3088).

Heronamide C diacetate (3a). A solution of **3** (3.5 mg) in pyridine (300 µL) and acetic anhydride (300 µL) was stirred overnight, after which the reaction was concentrated to dryness, resuspended in MeOH and purified by HPLC (Zorbax C_8 column, 250 × 9.4 mm, 5 µm, 4 mL min^{-1}, gradient from 10–100% MeOH–H_2O over 15 min, with a hold at 100% MeOH for 5 min) to yield the diacetate derivative **3a** (t_R = 17.2 min, 1.7 mg, 49%) as a yellow powder; $[\alpha]_D^{20}$ +519 (*c* 0.01, MeOH); UV (MeOH) λ_{max} (log ε) 230 (4.49), 290 (4.45); NMR (600 MHz, methanol-d_4) see ESI Table S6†; HRESI(+)MS *m/z* 55.3035 $(M+Na)^+$ (calcd for $C_{33}H_{43}NO_5Na$, 556.3033).

Heronamide A Mosher Analysis. A solution of **1a** (0.15 mg, 0.30 µmol), (*S*)-MTPA (1.5 mg, 6.4 µmol), DCC (2.0 mg, 9.7 µmol) and DMAP (2.0 mg, 16 µmol) in $CDCl_3$ (500 µL) was stirred at room temperature for 18 h. A second reaction was performed in an analogous manner using (*R*)-MTPA in place of (*S*)-MTPA. The products were analysed directly by NMR without further purification (ESI Fig. S7a†).

Cell Morphology Assay

HeLa cells were seeded in 96-well microtitre plates at 2 × 10^5 cells mL^{-1} in 100 µL of DMEM supplemented with 10% FBS and incubated for 6 h (37 °C; 5% CO_2). The cells were then treated, in triplicate, with either 10 µL of 10% DMSO (control) or 10 µL of heronamide C (500 µM in 10% DMSO) and incubated for a further 24 h (37 °C; 5% CO_2). After the second incubation, cells were imaged with a BD Pathway 855 bioimager using a 10× objective. Finally, the cells were exchanged into fresh media, incubated for a further 24 h (37 °C; 5% CO_2) and reimaged.

Acknowledgements

We thank M. Gauthier (UQ) for acquiring sediment samples, L. Sly and F. Lafi (UQ) for assistance in taxonomic analysis, and E. Lacey (BioAustralis, Sydney Australia) for support in scaled-up production of heronamide C. R.R. acknowledges the provision of an Australian Postgraduate Award. This research was funded in part by the Institute for Molecular Bioscience, The University of Queensland and the Australian Research Council.

References

1 R. Raju, A. M. Piggott, M. Conte, W. G. L. Aalbersberg, K. Feussner and R. J. Capon, *Org. Lett.*, 2009, **11**, 3862–3865.
2 R. Raju, A. M. Piggott, M. Conte, Z. Tnimov, K. Alexandrov and R. J. Capon, *Chem.–Eur. J.*, 2010, **16**, 3194–3200.
3 T. R. Hoye, C. S. Jeffrey and F. Shao, *Nat. Protoc.*, 2007, **2**, 2451–2458.
4 H. Muller, E. Bischoff, V.-B. Fiedler, K. Weber, B. Fugmann and B. Rosen, "Anti-inflammatory macrolactam (cyclamenol)", *Germany Pat.*, WO 94/06774, 1993.
5 H. Shitakawa, S. Nakajima, M. Hirayama, H. Kondo, K. Kojiri and H. Suda, "Antitumor substance, BE-67251, and its manufacture with Streptomyces species." *Japan Pat.*, JP 2000086664 A, 2000.

6 M. Nazare and H. Waldmann, *Tetrahedron Lett.*, 2000, **41**, 625–628.
7 M. Nazare and H. Waldmann, *Angew. Chem., Int. Ed.*, 2000, **39**, 1125–1128.
8 K. Kojiri, S. Nakajima, H. Suzuki, H. Kondo and H. Suda, *J. Antibiot.*, 1992, **45**, 868–874.
9 I. Takahashi, Y. Oda, Y. Nishiie, K. Ochiai and T. Mizukami, *J. Antibiot.*, 1997, **50**, 186–188.
10 K. Shindo, M. Kamishohara, A. Odagawa, M. Matsuoka and H. Kawai, *J. Antibiot.*, 1993, **46**, 1076–1081.
11 Y. Matsushima, H. Itoh, T. Nakayama, S. Horiuchi, T. Eguchi and K. Kakinuma, *J. Chem. Soc., Perkin Trans. 1*, 2002, 949–958.
12 Y. Matsushima, T. Nakayama, M. Fujita, R. Bhandari, T. Eguchi, K. Shindo and K. Kakinuma, *J. Antibiot.*, 2001, **54**, 211–219.
13 H. Joergensen, K. F. Degnes, A. Dikiy, E. Fjaervik, G. Klinkenberg and S. B. Zotchev, *Appl. Environ. Microbiol.*, 2010, **76**, 283–293.
14 S. S. Mitchell, B. Nicholson, S. Teisan, K. S. Lam and B. C. M. Potts, *J. Nat. Prod.*, 2004, **67**, 1400–1402.
15 D. W. Udwary, L. Zeigler, R. N. Asolkar, V. Singan, A. Lapidus, W. Fenical, P. R. Jensen and B. S. Moore, *Proc. Natl. Acad. Sci. U. S. A.*, 2007, **104**, 10376–10381.